Seismic Performance of Prefabricated Concrete Pier with Slot Connection

Sibo Su[1], Zhicong Li[2] and Guiman Liu[2]

[1]*School of civil engineering and transportation, Hebei University of technology, Tianjin 300401*
[2]*Hebei Provincial Communications Planning and Design Institute, Shijiazhuang 053001*

Keywords: Structural engineering, slot type, axial compression ratio, numerical simulation, seismic performance.

Abstract: In order to study the seismic performance of prefabricated concrete pier with slot connection, based on the Rongwu new line highway bridge project, this paper uses finite element analysis software ABAQUS to carry out the numerical simulation analysis of three kinds of fully prefabricated concrete pier with slot connection under different axial compression ratio, focusing on their bearing capacity, hysteretic characteristics, skeleton curve and ductility. Also, fully prefabricated slotted pier specimens were designed and manufactured to carry out the quasi-static test. The results show that with the increase of axial compression ratio, the bearing capacity of slotted pier increases gradually, while the failure rate of bearing capacity grows faster, and the ductility coefficient also decreases. When the axial compression ratio is about 0.2, fully prefabricated slotted pier has better seismic performance.

1. Introduction

In recent years, with the large-scale construction of the expressway network, the concept of bridge assembly has become more and more popular, and the prefabricated construction method of prefabricated bridge structures has been increasingly recognized by industry personnel[1]. For the prefabricated pier structure, the reliability of the connection between the column and the bent cap and the convenience of assembly are the key factors to choose the connection mode of the pier.

Slotted connection is to insert the pier reinforcement into the reserved hole of the prefabricated bent cap, which is composed of metal bellows and the reinforcement at the top and bottom, and it will be grouted after the installation of the prefabricated bent cap.

Compared with grouting sleeve connection, grouting bellows connection, socket connection, cast-in-place wet joint connection and other connection methods, the advantages of slot connection mainly include larger construction tolerance, smaller requirements for construction hoisting accuracy and component prefabrication accuracy, simple construction process, good structural integrity, reliable mechanical performance. It meets the requirements of China's construction habits, and the technical level of the construction workers is not high[2]. However, the diameter of the bellows used is very large, so it is necessary to cut off the reinforcement in the cover beam, which affects the mechanical and seismic performance of the pier column.

Redfish Bay Bridge in Texas in 1994 and Boone County IBRC Project Bridge in 2006 adopted this connection mode. In 2009, Erice. Matsumoto[5] conducted a quasi-static scale model test for

slotted connections. The test results show that the model has good bearing capacity. Wei Ying[6] introduced the application and difficulties of slot connection technology based on the bridge engineering in the reconstruction and expansion of Anhui section of JingTai expressway, but he did not make a detailed study on its seismic performance.

Summing up the research status of the existing prefabricated connection, it can be found that the domestic and foreign scholars have relatively little research on the seismic performance of slot connection. Therefore, this paper relies on the bridge project of Rongwu high-speed new line, with the help of quasi-static test and numerical simulation expansion analysis, focusing on the seismic performance of slot connection under different axial compression ratio, to improve reliability demonstration of construction technology and provide strong technical support for design.

2. Establishment of Finite Element Model

2.1.Model Design

Based on the general structural drawing of the bridge of Rongwu New Line, this paper uses ABAQUS to design prefabricated slot type piers with axial compression ratios of 0.3, 0.2 and 0.06 respectively, numbered S1, S2 and S3. The design of the three models adopts a uniform size, with a cap beam size of 2500mm × 1000mm × 1500mm and a pier shaft diameter of 900mm.

In order to facilitate the transportation of test specimens and save costs, considering that the transverse deformation of the pier is antisymmetric and the symmetrical center is the reverse bending point, so half of the pier height is taken for the pier which cut from the reverse bending point upward to the bent cap. Therefore, the designed pier height is 2000mm, corresponding to the actual pier height of 4000mm.

A 1100mm diameter metal corrugated pipe with a wall thickness of 1.6mm and a wave shape of 68mm × 13mm is reserved in the capping beam. The concrete strength grade of pier body and cover beam are both C60, the elastic modulus is 3.2 × 104mpa, HRB335 thread reinforcement is used, the diameter of longitudinal reinforcement of cover beam is 22mm, and the diameter of stirrup is 12mm. The diameter of the longitudinal reinforcement of the pier body is 20mm, the spiral hoop reinforcement has a spiral spacing of 100mm and a diameter of 6mm, the thickness of the concrete protective layer of the pier body is 55mm, and the cover beam is equipped with a steel mesh and 4 layers are arranged in the height direction. The grouting material in the metal bellows is high-strength non-shrinkage concrete. The connection design of the prefabricated model is shown in Figure 1, the reinforcement of the pier is shown in Figure 2, and the reinforcement of the cover beam is shown in Figure 3.

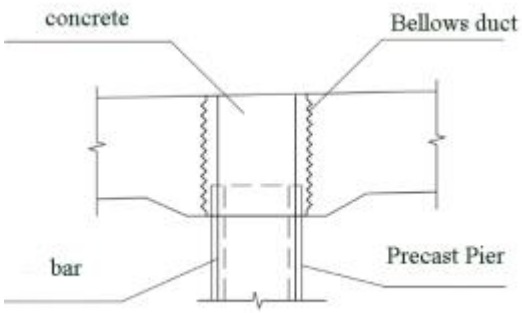

Figure 1: Slotted connection design diagram.

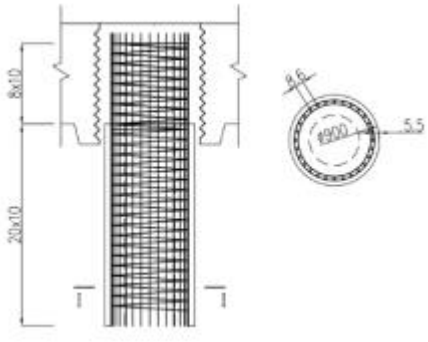

Figure 2: Reinforcement diagram of pier body.

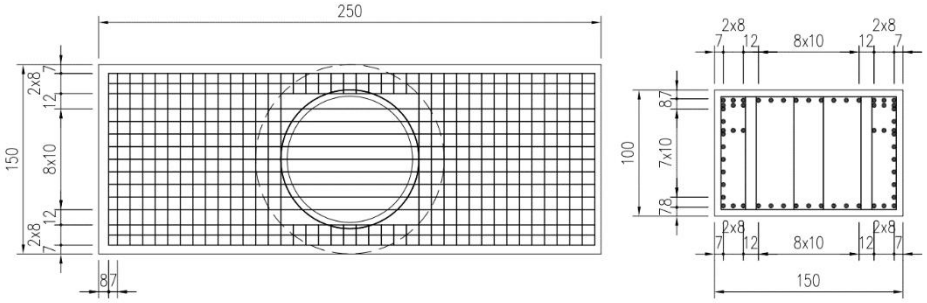

Figure 3: Reinforcement diagram of cover beam.

2.2.Selection of Element Type and Meshing

In the three models, the cover beams, pier columns, and grouts all use three-dimensional 8-node linear reduced integral units (C3D8R), the steel bars use 2-node linear three-dimensional truss elements (T3D2), and the metal bellows use shell elements (S4R)). It is assumed that there is no relative slip between reinforcement-concrete, reinforcement-grouting, grout-bellows, and bellows-concrete.

Finite element mesh division of bridge piers: the mesh size of grout, pier body and reinforcement is about 20cm, and the mesh size of cover beam is about 25cm. The structure of the bellows is more complicated, and the grid is divided into fine grids with a grid size of about 10cm. The finite element mesh model is shown in Figure 4, and the reinforcement skeleton is shown in Figure 5.

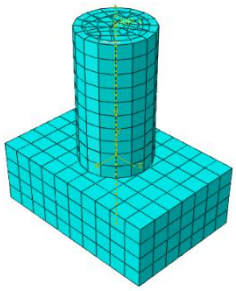

Figure 4: Finite element model.

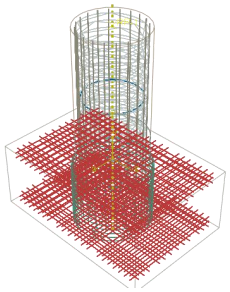

Figure 5: Finite element steel skeleton model.

2.3.Selection of Material Constitutive Relations

The constitutive model of concrete materials is the Concrete Damage Plastic Model (CDP), which can simulate mechanical properties of concrete stiffness recovery under reverse loading. It is a commonly used analysis model for concrete structures under cyclic loading; steel bars and metal bellows are both elastic-plastic constitutive model.

In the calculation of the concrete damage model, the concrete compression curve given in accordance with Chinese code is shown in equation (1):

$$\sigma_c = \begin{cases} f_c \dfrac{nx}{n-1+x^n} (x \le 1) \\ f_c \dfrac{x}{\alpha_c (x-1)^2 + x} (x > 1) \end{cases} \quad (1)$$

Where σ_c is the concrete stress; f_c is the concrete peak stress (concrete strength); $\alpha_c = 0.157 f_c^{0.785} - 0.905$; ε_c is the concrete strain; $x = \varepsilon_c / \varepsilon_0$; ε_0 is the strain corresponding to the peak stress; E_c is the elastic modulus; E_0 is the secant modulus corresponding to the peak stress; $n = E_c / (E_c - E_0)$. The material parameters of C60 are selected from the specification to obtain the basic parameters of the concrete damage model. The damage parameters are selected according to [7]. The calculation method of this damage factor is the damage evolution equation $\sigma = E_0 (1-d)\varepsilon$ proposed by Lematire: $d = (1-\sigma)/E_0 \varepsilon$. The value should be above 0.95. When selecting concrete compressive stress and inelastic damage data, the data must be manually intercepted. The starting point of the intercepting strain is 0.4 ε_0 and the ending point of the intercepting strain is 3 ε_0.

2.4.Loading System

The loading system mainly includes constant axial pressure and horizontal cyclic load. Select the loading method as inverted loading, set the coupling point on the top of the pier column, select the entire top surface of the pier column in the coupling area, and perform vertical axial force loading and horizontal loading on the coupling point. Two analysis steps are set during loading. The vertical force is applied in the first analysis step. According to the setting of different axial pressure ratios, the vertical force of the three models can be calculated to be 5245kN, 3497kN and 1100kN

respectively. In the second analysis step, the horizontal cyclic load is applied. Due to the small shear span and high rigidity of the pier, the use of conventional force-displacement control will cause large fluctuations in the force and even monotonic loading failure. Therefore, the horizontal load is used to achieve the test target force, loading system is shown in Figure 6. When the load reaches the specified displacement or the horizontal load drops below 85% of the maximum value, the load procedure stops.

2.5. Setting of Contact Action and Boundary Conditions

Since the prefabricated slotted pier is assembled [8], the phenomenon of opening and closing may occur under the load, which may cause the pressure distribution and friction to change with the load, so it is necessary to define a reasonable contact effect. When defining the complex contact between the pier and the cover beam, the normal behavior and the tangential behavior need to be defined separately. This model uses the Coulomb friction model to simulate the contact between the pier and the cover beam. Its normal behavior uses "hard contact", the size of the compressive stress transmitted between the contact surfaces is not limited; the tangential behavior uses "Frictional friction" , the contact surface is allowed to elastically slip. The coefficient of friction in each direction between the contact surfaces is 0.5 [9]. The contact between the reinforcement framework and the concrete is embedded, and the concrete hollow pier and the cavity are tied.

Because of the inverted loading method, in order to simulate the actual situation of the cover beam, the bottom end of the cover beam is set to be completely consolidated, and the directions outside the load (ie, the XY plane and the ZY plane) at the coupling point are set to restrict their rotation . The boundary conditions and contact conditions of the finite element model are shown in Figure 7.

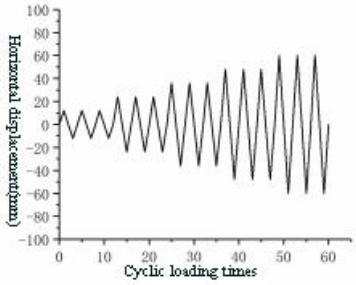

Figure 6: Horizontal loading system.

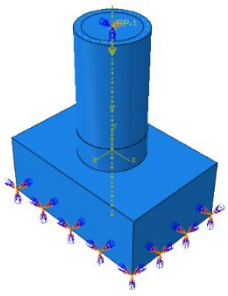

Figure 7: Constraints and contact conditions.

3. Quasi-static Test

3.1.Experimental Design

In order to verify the reliability of the finite element basic model, a full-scale model was designed in this paper, and the pseudo-static test of slotted pier was carried out at the Institute of Engineering Mechanics, China Earthquake Administration. The specimen number is S4, and all parameters of the test specimen are consistent with S3. The test was conducted under a large reaction force loading system. The loading system and loading method are consistent with the finite element model. The loading device is shown in Figure 8. The measurement system of the test is to collect the data of the strain gauges and displacement gauges of concrete and steel bars by the computer through the DH3815 dynamic and static strain test system. The displacement and force measurement of the top of the prefabricated pier column are collected by the system that comes with the servo loading, and the frequency of the collected data is 5Hz.

3.2.Test Phenomenon

According to Figure 9, the failure mode of S4 is mainly shear failure. At first, the bending shear oblique crack appeared in the test specimen, and then the crack developed diagonally downward, the slope increased continuously, and the crack area developed from the column foot upward to the loading height.

The joints and cover beams of the test piece did not produce substantial damage cracks throughout the test. When the loading force of the test piece was 74% of the maximum strength, radial micro cracks were generated at the place where the pier and cover beam were assembled. The sign of the end of the loading of the test piece is that the prefabricated pipe string has a wide X-shaped diagonal crack, and some of the cracks increase sharply in width, and develop into a critical diagonal crack, and the bearing capacity quickly drops to below 85% of the maximum value.

Figure 8: Test loading device.

Figure 9: Destruction of test specimen.

4. Comparison and Analysis of Results and Test Verification

4.1.Bearing Performance Analysis

It can be seen from Table 1 that the difference between the ultimate bearing capacity calculated by the numerical simulation and the test value is 12.6%, within 15%, the reliability of the model can be verified. This model can be used as the basis for the subsequent extended research on the axial compression ratio.

As shown in the table 1, with the increase of the axial compression ratio, the ultimate bearing capacity of the slotted pier increases and the ultimate displacement decreases. That is to say, after the structure has yielded, the bearing capacity stored is getting smaller and smaller, and the phenomenon of brittle failure is becoming more and more obvious. Although its ultimate bearing capacity continues to increase, the speed of reaching the ultimate bearing capacity is also getting faster and faster, so the ideal bearing performance can be obtained by controlling the axial compression ratio at about 0.2.

Table 1: Carrying performance.

parameter	S1	S2	S3	S4	Bearing capacity error of S3 and S4 /%
Horizontal displacement /mm	21.85	23.65	28.37	19.08	12.6%
Horizontal ultimate bearing capacity /kN	1257	1101	812	914	

4.2.Hysteresis Characteristics

It can be seen from Figure 11 that the shape of hysteresis curve, initial stiffness, loading stiffness, unloading stiffness, ultimate displacement and ultimate load of S3 and S4 are roughly consistent. From the comparison and analysis of S1, S2 and S3, with the increase of axial compression ratio, the initial stiffness and unloading stiffness of pier columns are also increasing, and the whole curve is gradually changing from the reverse S shape to the shuttle shape. When the axial compression ratio is about 0.1~0.2, the pier has obvious signs before failure, which is an ideal hysteretic curve in structural design. When the axial compression ratio reaches 0.3, the stiffness of pier increases obviously, and the failure mode is similar to that before, all of them are shear failure, but the structure has no obvious yield section, showing characteristics of brittle failure. The larger the axial compression ratio is, the higher the bearing capacity and yield load of the specimen are, but the worse the deformation capacity is when the specimen is damaged, the greater the loss of stiffness and the faster the failure speed of bearing capacity are. So when the axial compression ratio is about 0.2, the hysteretic curve is ideal.

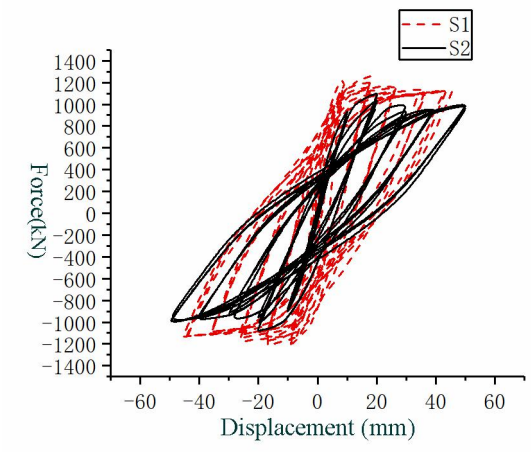

Figure 10: Comparison of S1 and S2 hysteretic curves.

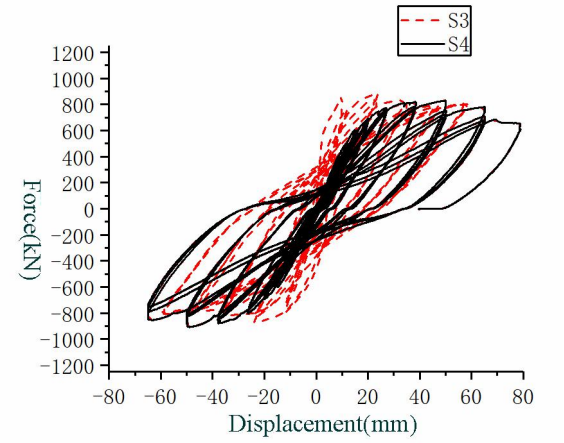

Figure 11: Comparison of S3 and S4 hysteretic curves.

4.3. Skeleton Curve

It can be seen from Figure 13 that the skeleton curves of S3 and S4 are roughly similar, and there is no obvious yield point. Through the comparison and analysis of S1, S2, and S3, with the increase of the axial compression ratio, the skeleton curve of the test piece becomes higher and steeper. When the axial compression ratio is 0.063, the ultimate displacement of the specimen is the largest, and the bearing capacity is the smallest. When the axial compression ratio increases from 0.06 to 0.2, the bearing capacity has been significantly improved. At the beginning of loading, the specimen is in the elastic stage. The initial stiffness of the specimen increases with the increase of the axial compression ratio. The initial stiffness of S2 and S1 is increased by 39.1kN/mm and 73.1kN compared to the initial stiffness of S3, respectively. 81.6% and 39.5%, it can be seen that when the axial compression ratio of the test piece is increased from 0.1 to 0.2, the initial stiffness is more obvious. When the axial compression ratio is increased from 0.2 to 0.3, the initial stiffness is not obvious. It shows that the larger axial compression ratio restricts the deformation capacity of the pier column and limits the development of pier column cracks, thereby greatly increasing the stiffness of the pier column. Therefore, when the axial compression ratio is selected as 0.2, the skeleton curve obtained is ideal.

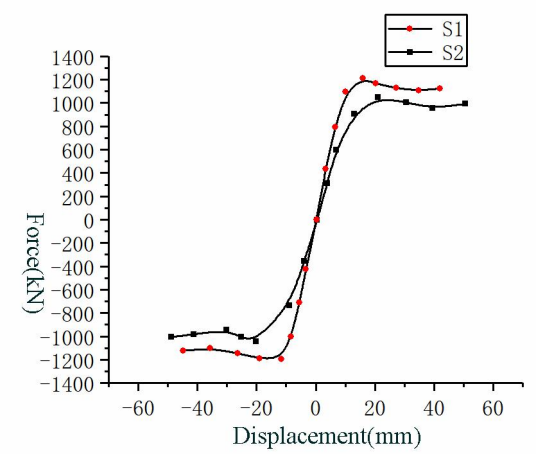

Figure 12: Comparison of S1 and S2 skeleton curves.

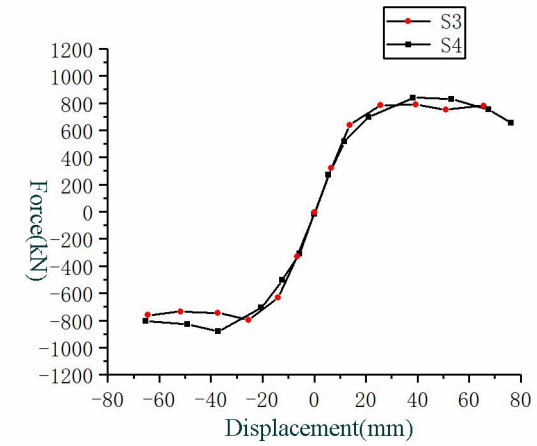

Figure 13: Comparison of S3 and S4 skeleton curves.

4.4.Ductility

Ductility refers to the ability of a structure to undergo inelastic deformation without significant degradation of initial strength. The ductility of members is mainly measured by the displacement ductility coefficient, which can be expressed as $\mu_{\Delta}=\frac{U_{\mathrm{m}}}{U_{\mathrm{y}}}$. Among them, U_{y} and U_{m} represent the yield displacement and limit displacement, respectively. However, there is no obvious yield displacement sign on the skeleton curve, and the yield point is difficult to determine, so this paper uses the equal energy method to approximate the yield displacement U_{y}. According to "Architectural Seismic Test Regulations" (JGJ/T10-2015), after the maximum load appears, the displacement corresponding to the maximum load when the load decreases with the deformation increases to 85% of the maximum load is the limit displacement U_{m}. The yield displacement, limit displacement and displacement ductility coefficients of the three models are determined according to the above method.

It can be seen from table 2 that the ductility coefficient of S2 and S1 is significantly lower than that of S3, the ductility coefficient of S2 is 42.2% lower than that of S3, and S1 is 26.7% lower than that of S2. When the axial compression ratio is 0.1-0.2, the specimen has better ductility. When the

axial compression ratio is increased to 0.3, the displacement ductility coefficient is reduced to 1.73, which is 46.3% lower than that when the axial compression ratio is 0.06. The downward trend is obvious. Therefore, it is recommended to choose the axial compression ratio of about 0.1-0.2, the test piece can have better ductility.

Table 2: Characteristic displacement and displacement ductility coefficient of the model.

	Yield displacement /mm	Ultimate displacement /mm	Displacement ductility coefficient
S1	23.33	40.38	1.73
S2	21.35	50.42	2.36
S3	19.22	61.90	3.22

5. Conclusions and Recommendations

In order to study the effect of axial compression ratio on the seismic performance of fully prefabricated slotted pier columns, three finite element models were established in this paper, finite element analysis and calculation were carried out, and the reliability of the finite element model was verified by a pseudo-static test. The following conclusions can be drawn:

(1) When the axial compression ratio of the slotted pier is 0.06~0.2, the structure has obvious yielding and strengthening sections during the loading process, and the failure forms are all shear failures, and there are no obvious signs of failure. With the increase of axial compression ratio, the bearing capacity of pier columns is getting larger and larger, and the failure speed of bearing capacity is getting faster and faster. After the axial pressure ratio is increased to 0.3, the phenomenon of brittle failure is more obvious.

(2) When the axial compression ratio is controlled at about 0.1~0.2, the slotted pier can obtain ideal hysteresis curve and skeleton curve. As the axial compression ratio increases, the larger axial force restricts the deformation of the test piece. Therefore, the initial stiffness of the specimen is gradually increased, and the ductility is gradually reduced. When the axial compression ratio is about 0.2, the seismic performance of the fully prefabricated slotted pier is optimal.

(3) Comparing the simulation results and the test results, it is found that the simulated hysteresis curve has a good fit with the curve obtained by the test, and the difference between the various data does not exceed 15%, indicating that the finite element model has the theory of the seismic performance of slotted pier The analysis is more accurate and can be used as the basis for further research.

(4) At present, there is relatively little research on slotted connection technology at home and abroad. Although its construction accuracy requirements are low, it also has the problem of cutting off the reinforcing steel in the cover beam, causing uneven force on the cover beam. In the future, the research on this connection method should be strengthened to formulate more reasonable and comprehensive special technical regulations.

References

[1] Zhanghua Xia, Jiping Ge, Zhouyang Yu, Yongbo He, Shangshun Lin. Two-way pseudo-static test of PC double-column piers assembled with grouted bellows [J]. China Journal of Highway and Transportation 2020,33(3): 1-14.(In Chinese)

[2] Wang Jingquan, Wang Zhen, Gao Yufeng, Zhu Junzheng. Research progress on seismic performance of prefabricated bridge pier system: new materials, new concepts, new applications [J]. Engineering Mechanics, 2019, 36(03): 1-23. (In Chinese)

[3] Brenes F J. Anchorage of grouted vertical duct connections for precast bent caps[D]. The University of Texas at Austin, Austin, 2005.

[4] Culmo M P. Connection details for prefabricated bridge elements and systems[R]. Report No. FHWA-IF-09-010, Federal Highway Administration, Washington, DC, 2009.

[5] Matsumoto E. Emulative precast bent cap connections for seismic regions: component tests report-preliminary grouted duct specimen (Unit 5). Report No. ECS-CSUS-2009-02. California State University, Sacramento, CA, 2010.

[6] Wei Ying, Fu Tingyang. Construction technology of fully prefabricated assembly of concrete bridges[J]. Urban Housing, 2018(6). (In Chinese)

[7] Fang Zihu, Zhou Haijun, Lai Shaoying, etc. ABAQUS concrete damage parameter calculation method[J], Building Structure, 2013(S2). (In Chinese)

[8] Chen Jinbiao. Research and application of connection performance between prefabricated hollow bridge pier and bearing cap of fabricated bridge [D]. Hefei: Hefei University of Technology, 2017. (In Chinese)

[9] Wang Jiejin, Huang Zhihua, Fu Kaimin. Finite element calculation and analysis of prefabricated bridge piers connected with grouted metal bellows[J]. Journal of Wuhan University of Technology (Transportation Science and Engineering Edition), 2019, 43(06): 1159-1164. (In Chinese)